Journal of Biomimetics, Biomaterials and Biomedical Engineering
ISSN: 2296-9845, Vol. 32, pp 98-114
doi:10.4028/www.scientific.net/JBBBE.32.98

Submitted: 2017-04-06
Revised: 2017-05-09
Accepted: 2017-05-10
Online: 2017-05-25

Prediction of Phagocyte Transmigration for Foreign Body Responses to Subcutaneous Biomaterial Implantations Using Differential Transform Method

Olurotimi Adeleye[1 *], Olatutu Olawale[2] and Gbeminiyi Sobamowo[3]

[1,2]Department of Systems Engineering, University of Lagos, Akoka, Lagos, Nigeria

[3]Department of Mechanical Engineering, University of Lagos, Akoka, Lagos, Nigeria

[1]rotimiadeleye1711@gmail.com, [2]olawaleolatutu@yahoo.com, [3]mikegbeminiyi@gmail.com

Keywords: Phagocyte transmigration; Foreign body response; Subcutaneous biomaterial implants; Differential transform method; Analytical solutions

Abstract. The complexity of the multiple interactive reactions of various cells/proteins and biochemical processes during phagocyte transmigration for foreign body responses to subcutaneous biomaterial implants have been studied through developed kinetics-based predictive models which have been numerically analyzed. However, the need for direct relationship between the kinetic-based predictive models parameters and the requirements for continuous insights into the significance of various process parameters affecting the phenomena have led to the quest for developing analytical solutions. Therefore, in this work, differential transform method is used to develop analytical solutions for the prediction of phagocyte transmigration for foreign body responses to subcutaneous biomaterial implants. The approximate analytical solutions are used to study the effect of various model parameters on phagocyte transmigration to foreign body responses in biomaterial implantation. The results of the analytical solutions are agreement with the results of the previous studies.

Introduction

The past few decades have witnessed and recorded remarkable developments and applications of biomaterials implants such as encapsulated tissues or cells, eye implants, neural electrodes and breast implants which cannot be overemphasized. One of such implant materials is the Zwitterionic hydrogel as used in an experiment on mice [1] (See Fig. 1). In the meantime, there are an increasing number of medical implants failures due to excessive fibrotic responses. Indisputably, implanted biomaterials provoke acute and chronic inflammatory responses, [2,3] which involve mechanisms such as phagocyte transmigration through the endothelial barrier, chemotaxis toward the implant, and phagocyte adherence to implant surfaces. These inflammatory responses may, in turn, presage serious iatrogenic consequences, such as the "hardening" and degradation of mammary implants [3,4], stress cracking of pacemaker leads [4-6], and fibrous thickening surrounding many types of implants. As one of the major factors comprising phagocyte transmigration, previous studies hypothesized that histamine might play an important role in the recruitment of inflammatory cells to implants [2]. On studying the foreign body reaction, a number of researches have been conducted for modeling and predicting foreign body fibrotic reactions. [5] proposed a hybrid model by combining a differential equation and kinetics Monte Carlo algorithm to simulate and predict phagocyte responses at molecular level. In few years later, [7] adapted chemical kinetic equations for building a predictive tool of foreign body fibrotic reactions while [8] utilized partial differential equations which were also utilized for macrophage spatial /temporal dynamics in foreign body reactions. In a study carried out by [9], investigation was done on the early foreign-body response in mice that could not synthesize complement and mice that could not synthesize immunoglobulin. In the work, it was found that such animals retained the ability to surround the implanted material with a layer of phagocytes (neutrophils and macrophages).

Figure 1: Components of (a) PCBMA and (b) PHEMA hydrogels and H&E stain images of samples implanted subcutaneously in mice for one week.

On the study of foreign body responses, [10-12], pointed out that the degree and extent of the FBR depends on the properties of the device, such as (a) composition, (b) contact duration, (c) degradation rate, (d) morphology, (e) porosity, (f) roughness, (g) shape, (h) size, (i) sterility, and (j) surface chemistry. In the earlier study, [13] stated that the chronic inflammation is histologically less uniform when compared to acute inflammation, and the wound healing response is generally dependent on the size and/or degree of injury. This phase is generally characterized by the presence of monocytes, macrophages, and lymphocytes, as well as the proliferation of blood vessels and connective tissue to restructure the affected area. Also, [14-17] submitted that the formation of blood vessels is essential to wound healing, supplying necessary nutrients. [15] pointed out that the extracellular matrix (ECM) acts not only as a physical scaffold but also as a crucial modulator of the biological processes, including differentiation, development regeneration, repair, as well tumor progression.

Despite the intensive research on determining the mechanisms governing such complex responses, few mechanistic mathematical models have been developed to study such foreign body reactions. The developed kinetics-based predictive models have been analyzed numerically to investigate the outcomes of multiple interactive complex reactions of various cells/proteins and biochemical processes and to understand transient behavior during the entire period (up to several months). However, the numerical solutions failed to symbolically show the direct relationship between the models parameters and could not also provide good and continuous insights into the significance of various process parameters affecting the phenomena. Therefore, in this work, differential transform method was applied to provide analytical solution to phagocyte transmigration for foreign body responses to subcutaneous biomaterial implants. Such a very powerful, novel and accurate approximate analytical solution provides symbolic solution which shows direct relationship between the models parameters and also provide good and continuous insights into the significance of various process parameters affecting the phenomena.

Differential transform method is an approximate analytical method for solving differential equations. Most of the analytical (exact or approximation) and purely numerical methods are computationally intensive or required symbolic computation for the calculation of higher order derivatives as in Taylor's method. Although, this concept was introduced by [16], its applications to both linear and non-linear differential and system of differential equation have fast gained ground or appeared in many engineering and scientific research. It is a semi-analytical technique that depends on Taylor's Series [17] and can solve differential equations, difference equation, differential-difference equations, fractional differential equation, pantograph equation and integro-differential equation. The method is applied to solve many non-linear integral and differential equations without linearization, discretization or perturbation and with high accuracy. DTM reduces the computational difficulties of the other traditional methods and also the calculations can be made with simple manipulations [18]. It provides more accurate solution or result than Variation Iteration Method (VIM) [19]). Also, DTM can be used to solve linear and non-linear non-homogeneous PDEs with accurate approximation, which is acceptable for small range, because of boundary conditions which are satisfied via the method (DTM), and the remaining unsatisfied conditions play no roles in the final results [20,22]. Laplace transform could be combined with the DTM to overcome this

deficiency that is mainly caused by the unsatisfied conditions [23]. DTM does not require many computations as carried out in ADM and VIM to have high and fast rate of convergence. An analytical expression as done in DTM is more convenient for engineering calculations as compared with experimental or numerical studies and is also obvious starting point for a better understanding of the relationship between the physical quantities. This semi-analytical solution/method would provide continuous physical insights than pure numerical computation/method.

Theoretical Background of the Phagocyte Transmigration

Medical implants provoke unpredicted responses and reactions of the immune system, which are fibrotic capsule formations surrounding the medical device. In view of the inert and nontoxic nature of most biomaterials, it is puzzling that tissue contact implants very often acquire an extensive overlay of phagocytic cells. These phagocytes have been implicated in a number of subsequent adverse effects such as osteolytic changes around joint implants, stress cracking of pacemaker leads, degradation of biomaterial implants. Indisputably, the retention of foreign bodies leads to the formation of a dense, hypocellular, collagen-rich capsule. This foreign-body capsule (FBC) is advantageous to the patient in many cases. For example, in a study of patients who retained lead bullet fragments, plumbism (clinical lead poisoning) was very rarely found. Hence, in attempting to define the mechanisms involved in biomaterial-mediated inflammatory responses, we have somewhat arbitrarily divided the events into (i) Phagocyte transmigration through the endothelial barrier, (ii) chemotaxis toward the implant, and (iii) phagocyte adherence to implant surfaces.

Mathematical Models of the Dynamics of Phagocyte Transmigration

The mathematical models are developed for the dynamics of phagocyte transmigration using rate/kinetics law models are developed

Residual Histamine. Based on biological measurement, it is legitimate to assume that the temporal residual histamine may have a regular pattern. In the biological sense, the phenomenon that residual histamine decreases dramatically for the first two hours can be described as residual histamine's degranulation from mast cells for histamine releasing. With the decreasing of residual histamine, another reasonable assumption is that the number of new mast cells is increased by an unknown external source after two hours. For this reason, the external source is modeled by a damped harmonic oscillator as given by [12,21] as

$$\ddot{U}_{xrmc}(t) + \beta \dot{U}_{xrmc}(t) + \omega_0^2(t) U_{xrmc}(t) = 0 \tag{1}$$

Where U_{xrmc} is the function of the external input source to release new mast cells, β is a non-negative constant for resistance of friction and mass, and $\omega_0$indicates the oscillator frequency.
Considering biological half-life cycle, residual histamine can be modeled by the following equation,

$$\dot{C}_{rh}(t) = -k_{rhch} C_{rh}(t) + U_{xrmc}(t) \tag{2}$$

Where $C_{rh}(t)$ is the concentration function of residual histamine, $k_{rhch}$is the rate that residual histamine decayed, and $U_{xrmc}(t)$ is the input function defined above.

Histamine. The concentration of histamine is increased as much as residual histamine's decreasing.

$$\dot{C}_h(t) = k_{rhch} C_{rh}(t) I_{mc}(t) - k_{hs} C_h(t) \tag{3}$$

Where $C_h(t)$ is the concentration function of histamine, k_{rhch} is the rate that histamine released from residual histamine given from residual histamine in Eq. (2), k_{hs} is the rate that histamine regulates itself, and $I_{mc}(t)$ is an input parameter indicating block/non-block mast cells. The first term on the right hand side of Eq. (3) represents the increasing of histamine released from mast cells. The second term on the right hand side of Eq. (3) represents the decay of histamine itself.

Histamine Receptor and Selectins. Histamine receptors enhance the permeability of the endothelial cell barrier of capillaries for phagocyte to transmigrate into the peritoneal space. It is modeled as,

$$\dot{C}_{hr}(t) = \frac{k_{hchrt} C_h(t)}{k_{hchrb} + C_h(t)} - k_{hrs} C_h(t) \tag{4}$$

Where $C_{hr}(t)$ is the concentration function of histamine receptors, $k_{hchrt}$and k_{hchrb} are the rate bounds that histamine receptors are combined by histamine, $k_{hrs}$is the rate that histamine receptors regulate themselves. In a similar way, selectins are modeled as,

$$\dot{C}_s(t) = \frac{k_{hcst} C_h(t)}{k_{hcsb} + C_h(t)} - k_{ss} C_s(t) \tag{5}$$

Where $C_s(t)$ is the concentration function of selectins, $k_{hcsb}$and k_{hcst} are the rate bounds for hyperbolic form, k_{ss} is the rate that selectins regulate themselves.

Phagocytes. For modeling of polymorphonuclear neutrophils (PMN) and monocytes/macrophages (MΦ), we consider capillary permeabilities for both of them, which are related to the transmigration rate of phagocytes,

$$\dot{C}_{pmnp}(t) = \frac{k_{pmnipt} C_{hr}(t) C_s(t) I_{pmns}(t) I_{pmnhr}(t)}{k_{pmnipb} + C_{hr}(t) C_s(t) I_{pmns}(t) I_{pmnhr}(t)} - k_{pmnps} C_{pmnp}(t) \tag{6}$$

where $C_{pmnp}(t)$ is the capillary permeability function for PMN to move into peritonea, k_{pmnipb} and $k_{pmnipt}$are the rate bounds for histamine receptors and selectins to increase permeability for PMN, $C_{hr}(t)$ is the concentration function of histamine receptors, $C_s(t)$ is the concentration function of selectins, $k_{pmnps}$is the contraction rate of capillary permeability, $I_{pmnhr}(t)$ is the input indicating block/unblock histamine receptors, and $I_{pmns}(t)$ is the input indicating block/un-block selectins. Similarly, the permeability function for MΦ can be modeled as,

$$\dot{C}_{mpp}(t) = \frac{k_{mpipt} C_{hr}(t) C_s(t) I_{mps}(t) I_{mphr}(t)}{k_{mpipb} + C_{hr}(t) C_s(t) I_{mps}(t) I_{mphr}(t)} - k_{mpps} C_{mpp}(t) \tag{7}$$

Where $C_{mpp}(t)$ is the capillary permeability function for MΦ to move into peritonea, k_{mpipb} and k_{mpipt} are the rates for histamine receptors and selectins to increase permeability for MΦ, and k_{mpps} is the contraction rate of capillary permeability. Now we can model the recruited PMN as,

$$\dot{C}_{pmn}(t) = C_{pmnp}(t) - k_{pmns} C_{pmn}(t) \tag{8}$$

Where $C_{pmn}(t)$ is the concentration function of PMN, C_{pmnp} is the permeability for PMN, k_{pmns} is the rate of self-degradation. Now we can model the recruited MΦ as,

$$\dot{C}_{mp}(t) = C_{mpp}(t) - k_{mps} C_{mp}(t) \tag{9}$$

Where $C_{mp}(t)$ is the concentration function of MΦ, C_{mpp} is the permeability for MΦ, k_{mps} is the rate of self-degradation.

Method of solution: Differential transforms method

In this work, differential transform method is used to solve nonlinear equations in Eqs. (1-9). The basic definitions of the method is as follow

Basic definition of differential transform method. If $u(t)$ is analytic in the domain T, then it will be differentiated continuously with respect to time *t.*

$$\frac{d^p u(t)}{dt^p} = \varphi(t, p) \quad \text{for} \quad \text{all } t \in T \tag{10}$$

For $t = t_i$, then $\varphi(t, p) = \varphi(t_i, p)$, where p belongs to the set of non-negative integers,denoted as the p-domain. Therefore Eq. (10) can be rewritten as

$$U(p) = \varphi(t_i, p) = \left[\frac{d^p u(t)}{dt^p} \right]_{t=t_i} \tag{11}$$

Where U_p is called the spectrum of $u(t)$ at $t = t_i$

If $u(t)$ can be expressed by Taylor's series, the $u(t)$ can be represented as

$$u(t) = \sum_{p}^{\infty} \left[\frac{(t-t_i)^p}{p!} \right] U(p) \tag{12}$$

Where Equ. (11) is called the inverse of $U(k)$ using the symbol 'D' denoting the differential transformation process and combining Eqs. (9) and (10), it is obtained that

$$u(t) = \sum_{p=0}^{\infty} \left[\frac{(t-t_i)^p}{p!} \right] U(p) = D^{-1}U(p) \tag{13}$$

Operational properties of differential transformation method. If $u(t)$ *and* $v(t)$ are two independent functions with time (t) where $U(p)$ and $V(p)$ are the transformed function corresponding to $u(t)$ and $v(t)$, then it can be proved from the fundamental mathematics operations performed by differential transformation that.

i. If $z(t) = u(t) \pm v(t)$, then $Z(p) = U(p) \pm V(p)$

ii. If $z(t) = \alpha u(t)$, then $Z(p) = \alpha U(p)$

iii. If $z(t) = \dfrac{du(t)}{dt}$, then $Z(p) = (p-1)\,U(p+1)$

iv. If $z(t) = u(t)v(t)$, then $Z(t) = \sum_{r=0}^{p} V(r)U(p-r)$

v. If $z(t) = u^m(t)$, then $Z(t) = \sum_{r=0}^{p} U^{m-1}(r)U(p-r)$

vi. If $z(t) = u(t)v(t)$, then $Z(k) = \sum_{r=0}^{p} (r+1)V(r+1)U(p-r)$

Analytical Solution Procedures

The analytical solutions of the linear Eqs. (1-3)

$$U(t) = k_{eo1}e^{-k_{k1}t} + \gamma k_{eo11}e^{-(k_{k1}+\beta)t} \cos\left(\sqrt{1-\beta^2}te^{-k_{k2}t}\right) \tag{14}$$

Where

$$A(t) = k_{eo1}e^{-k_{k1}(t-t_1)} \qquad \omega_0(t) = k_{wo}e^{-k_{k2}(t-t_1)}$$

$$k_{eo1} = k_{eo}e^{k_{k1}t_1} \qquad k_{eo11} = k_{eo1}e^{-\beta t_1} \qquad \gamma = k_{wo}t_1e^{k_{k2}t_1}$$

Also

$$C_2 = e^{-k_r t}\int\left[k_{eo1}e^{(k_r-k_{k1})t} + \gamma k_{eo11}e^{(k_r-k_{k1}-\beta)t}\cos\left(\overline{\gamma}te^{-k_{k2}t}\right)\right] \tag{15}$$

And

$$C_3 = k_r I_{mc}e^{-k_h t}\int\left\{e^{-k_h t}\int\left[k_{eo1}e^{(k_r-k_{k1})t} + \gamma k_{eo11}e^{(k_r-k_{k1}-\beta)t}\cos\left(\overline{\gamma}te^{-k_{k2}t}\right)\right]\right\} \tag{16}$$

Where

$$\overline{\gamma} = \gamma\sqrt{1-\beta^2}, \qquad h = k_r - k_{k1} - \beta,\ a = -k_{k2} \tag{17}$$

The nonlinear Eq. (4)-(9) are solved by using DTM
Therefore, on carrying out the differential transform of Eq. (4) – (9), we have the following recursive equations.

$$k_{4a}(k+1)C_4(k+1) + \sum_{l=0}^{k}(l+1)C_4(l+1)C_3(k-l) = k_{4b}C_3(k) - k_{4c}k_{4a}C_4(k) - k_{4c}\sum_{l=0}^{k}C_4(l)C_3(k-l) \tag{18}$$

$$k_{5a}(k+1)C_5(k+1) + \sum_{l=0}^{k}(l+1)C_5(l+1)C_3(k-l) = k_{5b}C_3(k) - k_{5c}k_{5a}C_5(k) - k_{5c}\sum_{l=0}^{k}C_5(l)C_3(k-l) \tag{19}$$

$$k_{6a}(k+1)C_6(k+1) + I_{6a}I_{6b}\sum_{l=0}^{k}\sum_{p=0}^{k-l}(l+1)C_6(l+1)C_5(p)C_4(k-l-p) = k_{6b}I_{6a}I_{6b}\sum_{l=0}^{k}C_5(l)C_4(k-l) - k_{6a}k_{6c}C_6(k) - k_{6c}I_{6a}I_{6b}\sum_{l=0}^{k}\sum_{p}^{k-l}C_6(l)C_5(p)C_4(k-l-p) \tag{20}$$

$$k_{7a}(k+1)C_7(k+1) + I_{7a}I_{7b}\sum_{l=0}^{k}\sum_{p=0}^{k-l}(l+1)C_7(l+1)C_5(p)C_4(k-l-p) = k_{7b}I_{7a}I_{7b}\sum_{l=0}^{k}C_5(l)C_4(k-l) - k_{7a}k_{7c}C_7(k) - k_{7c}I_{7a}I_{7b}\sum_{l=0}^{k}\sum_{p}^{k-l}C_7(l)C_5(p)C_4(k-l-p) \tag{21}$$

$$C_8(k+1) = \frac{1}{k+1}\left(C_6(k) - k_8C_8(k)\right) \tag{22}$$

$$C_9(k+1) = \frac{1}{k+1}\left(C_7(k) - k_9C_9(k)\right) \tag{23}$$

The analyses of the transform form of the above equations are as follows
For Eq. (18)

$$k_{4a}(k+1)C_4(k+1) + \sum_{l=0}^{k}(l+1)C_4(l+1)C_3(k-l) = k_{4b}C_3(k) - k_{4c}k_{4a}C_4(k) - k_{4c}\sum_{l=0}^{k}C_4(l)C_3(k-l)$$

When

$k = 0$

$$C_4(1) = \frac{1}{\left(k_{4a} + C_3(0)\right)}\left(k_{4b}C_3(0) - k_{4c}k_{4a}C_4(0) - k_{4c}C_4(0)C_3(0)\right)$$

$k = 1$

$$C_4(2) = \frac{1}{2\left(k_{4a} + C_3(0)\right)}\left(k_{4b}C_3(1) - k_{4c}k_{4a}C_4(1) - k_{4c}\left(C_4(0)C_3(1) + C_4(1)C_3(0)\right) - C_4(1)C_3(1)\right)$$

$k=2$

$$C_4(3)=\frac{1}{3\left(k_{4a}+C_3(0)\right)}\begin{pmatrix}k_{4b}C_3(2)-k_{4c}k_{4a}C_4(2)-k_{4c}\left(C_4(0)C_3(2)+C_4(1)C_3(1)+C_4(2)C_3(0)\right)\\-C_4(1)C_3(2)-2C_4(2)C_3(1)\end{pmatrix}$$

$k=3$

$$C_4(4)=\frac{1}{4\left(k_{4a}+C_3(0)\right)}\begin{pmatrix}k_{4b}C_3(3)-k_{4c}k_{4a}C_4(3)-k_{4c}\left(C_4(0)C_3(3)+C_4(1)C_3(2)+C_4(2)C_3(1)+C_4(3)C_3(0)\right)\\-C_4(1)C_3(3)-2C_4(2)C_3(2)-3C_4(3)C_3(1)\end{pmatrix}$$

$k=4$

$$C_4(5)=\frac{1}{5\left(k_{4a}+C_3(0)\right)}\begin{pmatrix}k_{4b}C_3(4)-k_{4c}k_{4a}C_4(4)-k_{4c}\left(C_4(0)C_3(4)+C_4(1)C_3(3)+C_4(2)C_3(2)+C_4(3)C_3(1)+C_4(4)C_3(0)\right)\\-C_4(1)C_3(4)-2C_4(2)C_3(3)-3C_4(3)C_3(2)-4C_4(4)C_3(1)\end{pmatrix}$$

$k=5$

$$C_4(6)=\frac{1}{6\left(k_{4a}+C_3(0)\right)}\begin{pmatrix}k_{4b}C_3(5)-k_{4c}k_{4a}C_4(5)-k_{4c}\left(C_4(0)C_3(5)+C_4(1)C_3(4)+C_4(2)C_3(3)+C_4(3)C_3(2)+C_4(4)C_3(1)+C_4(5)C_3(0)\right)\\-C_4(1)C_3(5)-2C_4(2)C_3(4)-3C_4(3)C_3(3)-4C_4(4)C_3(2)-5C_4(5)C_3(1)\end{pmatrix}$$

$k=6$

$$C_4(7)=\frac{1}{7\left(k_{4a}+C_3(0)\right)}\begin{pmatrix}k_{4b}C_3(6)-k_{4c}k_{4a}C_4(6)-k_{4c}\begin{pmatrix}C_4(0)C_3(6)+C_4(1)C_3(5)+C_4(2)C_3(4)+C_4(3)C_3(3)+\\C_4(4)C_3(2)+C_4(5)C_3(1)+C_4(6)C_3(0)\end{pmatrix}\\-C_4(1)C_3(6)-2C_4(2)C_3(5)-3C_4(3)C_3(4)-4C_4(4)C_3(3)-5C_4(5)C_3(2)-6C_4(6)C_3(1)\end{pmatrix}$$

Following the definition of inverse DTM as given by Eq.(13), we have

$$C_4(t)=C_4(0)+tC_4(1)+t^2C_4(2)+t^3C_4(3)+t^4C_4(4)+t^5C_4(5)+t^6C_4(6)+t^7C_4(7) \tag{24}$$

Also, the analysis of Eq. (19) is as shown as follows

$$k_{5a}(k+1)C_5(k+1)+\sum_{l=0}^{k}(l+1)C_5(l+1)C_3(k-l)=k_{5b}C_3(k)-k_{5c}k_{5a}C_5(k)-k_{5c}\sum_{l=0}^{k}C_5(l)C_3(k-l)$$

When

$k=0$

$$C_5(1)=\frac{1}{\left(k_{5a}+C_3(0)\right)}\left(k_{5b}C_3(0)-k_{5c}k_{5a}C_5(0)-k_{5c}C_5(0)C_3(0)\right)$$

$k=1$

$$C_5(2)=\frac{1}{2\left(k_{5a}+C_3(0)\right)}\left(k_{5b}C_3(1)-k_{5c}k_{5a}C_5(1)-k_{5c}\left(C_5(0)C_3(1)+C_5(1)C_3(0)\right)-C_5(1)C_3(1)\right)$$

$k=2$

$$C_5(3)=\frac{1}{3\left(k_{5a}+C_3(0)\right)}\begin{pmatrix}k_{5b}C_3(2)-k_{5c}k_{5a}C_5(2)-k_{5c}\left(C_5(0)C_3(2)+C_5(1)C_3(1)+C_5(2)C_3(0)\right)\\-C_5(1)C_3(2)-2C_5(2)C_3(1)\end{pmatrix}$$

$k=3$

$$C_5(4)=\frac{1}{5\left(k_{5a}+C_3(0)\right)}\begin{pmatrix}k_{5b}C_3(3)-k_{5c}k_{5a}C_5(3)-k_{5c}\left(C_5(0)C_3(3)+C_5(1)C_3(2)+C_5(2)C_3(1)+C_5(3)C_3(0)\right)\\-C_5(1)C_3(3)-2C_5(2)C_3(2)-3C_5(3)C_3(1)\end{pmatrix}$$

$k=4$

$$C_5(5)=\frac{1}{5\left(k_{5a}+C_3(0)\right)}\begin{pmatrix}k_{5b}C_3(4)-k_{5c}k_{5a}C_5(4)-k_{5c}\left(C_5(0)C_3(4)+C_5(1)C_3(3)+C_5(2)C_3(2)+C_5(3)C_3(1)+C_5(4)C_3(0)\right)\\-C_5(1)C_3(4)-2C_5(2)C_3(3)-3C_5(3)C_3(2)-4C_5(4)C_3(1)\end{pmatrix}$$

$k = 5$

$$C_5(6) = \frac{1}{6(k_{5a} + C_3(0))} \begin{pmatrix} k_{5b}C_3(5) - k_{5c}k_{5a}C_5(5) - k_{5c}\left(C_5(0)C_3(5) + C_5(1)C_3(4) + C_5(2)C_3(3) + C_5(3)C_3(2) + C_5(4)C_3(1) + C_5(5)C_3(0)\right) \\ -C_5(1)C_3(5) - 2C_5(2)C_3(4) - 3C_5(3)C_3(3) - 4C_5(4)C_3(2) - 5C_5(5)C_3(1) \end{pmatrix}$$

$k = 6$

$$C_5(7) = \frac{1}{7(k_{5a} + C_3(0))} \begin{pmatrix} k_{5b}C_3(6) - k_{5c}k_{5a}C_5(6) - k_{5c}\begin{pmatrix} C_5(0)C_3(6) + C_5(1)C_3(5) + C_5(2)C_3(4) + C_5(3)C_3(3) + \\ C_5(4)C_3(2) + C_5(5)C_3(1) + C_5(6)C_3(0) \end{pmatrix} \\ -C_5(1)C_3(6) - 2C_5(2)C_3(5) - 3C_5(3)C_3(4) - 4C_5(4)C_3(3) - 5C_5(5)C_3(2) - 6C_5(6)C_3(1) \end{pmatrix}$$

Using the definition of inverse DTM as given by Eq.(13), we have

$$C_5(t) = C_5(0) + tC_5(1) + t^2C_5(2) + t^3C_5(3) + t^4C_5(4) + t^5C_5(5) + t^6C_5(6) + t^7C_5(7) \tag{25}$$

Also, Eq. (20)-(23) are analyzed in the same way

Table 1: Estimated parameters by DSLM [24].

Parameter	Description	Estimation
t_1	Starting time that the external source is released	3.5000
k_{e0}	An initial concentration of the external source	11.2464
k_{k1}	A self contraction of the external source	0.1017
β	An initial concentration of the oscillation of the oscillation bound	0.0134
k_{w0}	An initial value of the oscillation frequency	1.4037
k_{k2}	A contraction rate of the oscillation frequency	0.0937
k_{rhch}	A rate that the residual histamine decayed	0.3704
k_{hs}	A rate that the histamine regulates itself	0.0002
k_{hchrb}	A rate that the histamine receptors are released	0.9997
k_{hchrt}	A upper bound rate that the histamine receptors are released	0.0757
k_{hrs}	A rate that the histamine receptors regulate themselves	0.7232
k_{hcsb}	A lower bound of rate that the selectins are released	1.9997
k_{hcst}	A upper bound of rate that the selectins are released	0.2668
k_{ss}	A rate that the selectins regulate themselves	0.1024
k_{pmnipb}	A lower bound of rate that increases the permeability for PMN	0.2226
k_{pmnipt}	A upper bound of rate that increases the permeability for PMN	2.0000
k_{pmnps}	A rate that the permeability of the capillary self degrades	0.1003
k_{mpipb}	A lower bound of rate that increases the permeability for Mϕ	0.0001
k_{mpipt}	A upper bound of rate that increases the permeability for Mϕ	1.0108
k_{mpps}	A rate that the permeability of the capillary self degrades	0.1961
k_{mpns}	A rate that the PMN self degrades	0.0582
k_{mps}	A rate that the Mϕself degrades	0.0307

Results and Discussion

The result of the developed models simulations are presented in Fig. 2-8

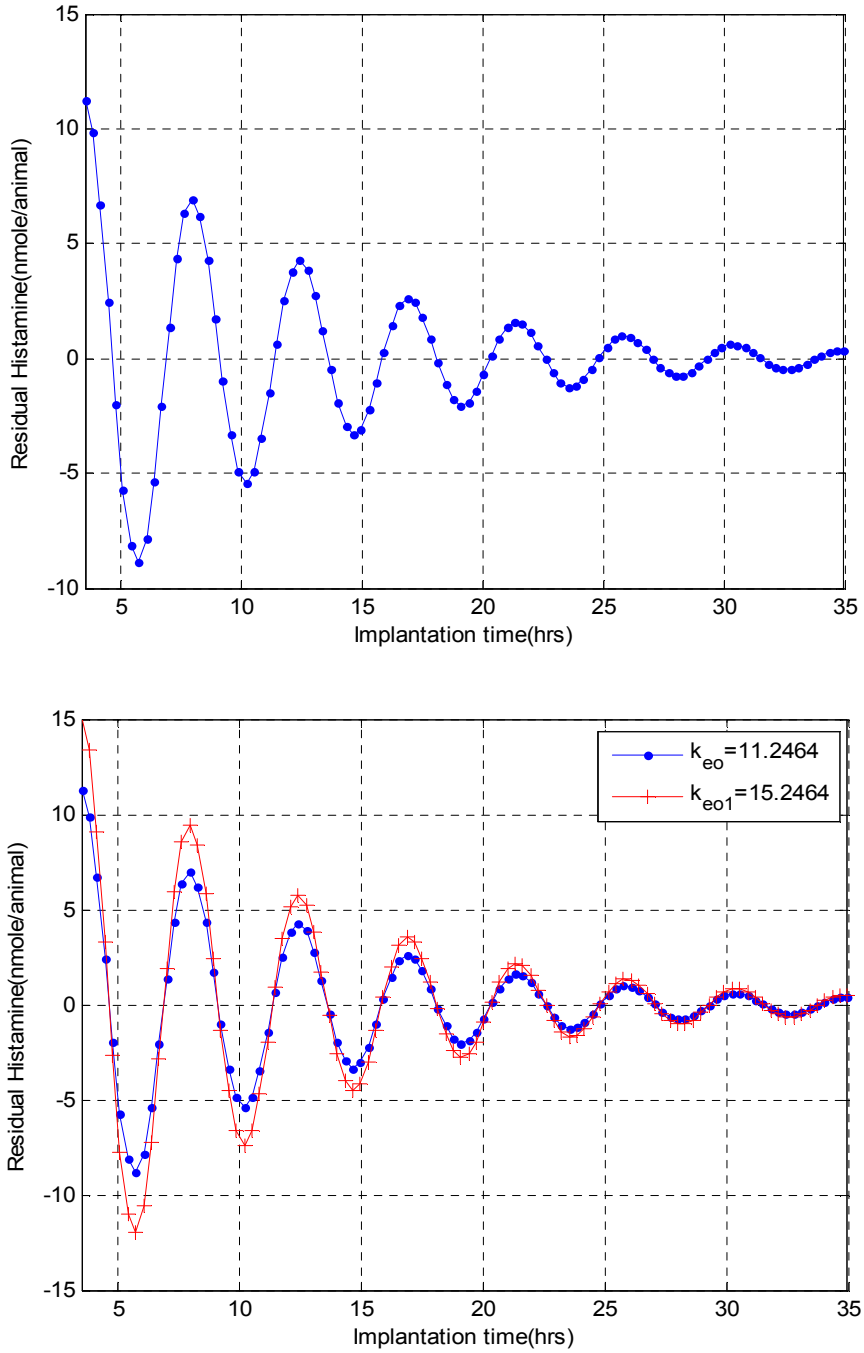

Figure 2: (a) Variation of residual histamine with implantation time; (b) Effects of the initial concentration of the external source on residual histamine.

Fig. 2 (a) shows the variation of residual histamine with implantation under damped oscillation and time-invariant condition of the oscillatory frequency. The damping nature of the residual histamine with time is recorded due to the non-negative constant for the resistance of friction and mass. The effect if initial concentration of the external source on residual histamine is depicted in Fig 2(b) From the result, it shows that the residual histamine increase with increase in initial concentration of the external source under time-invariant oscillation frequency.

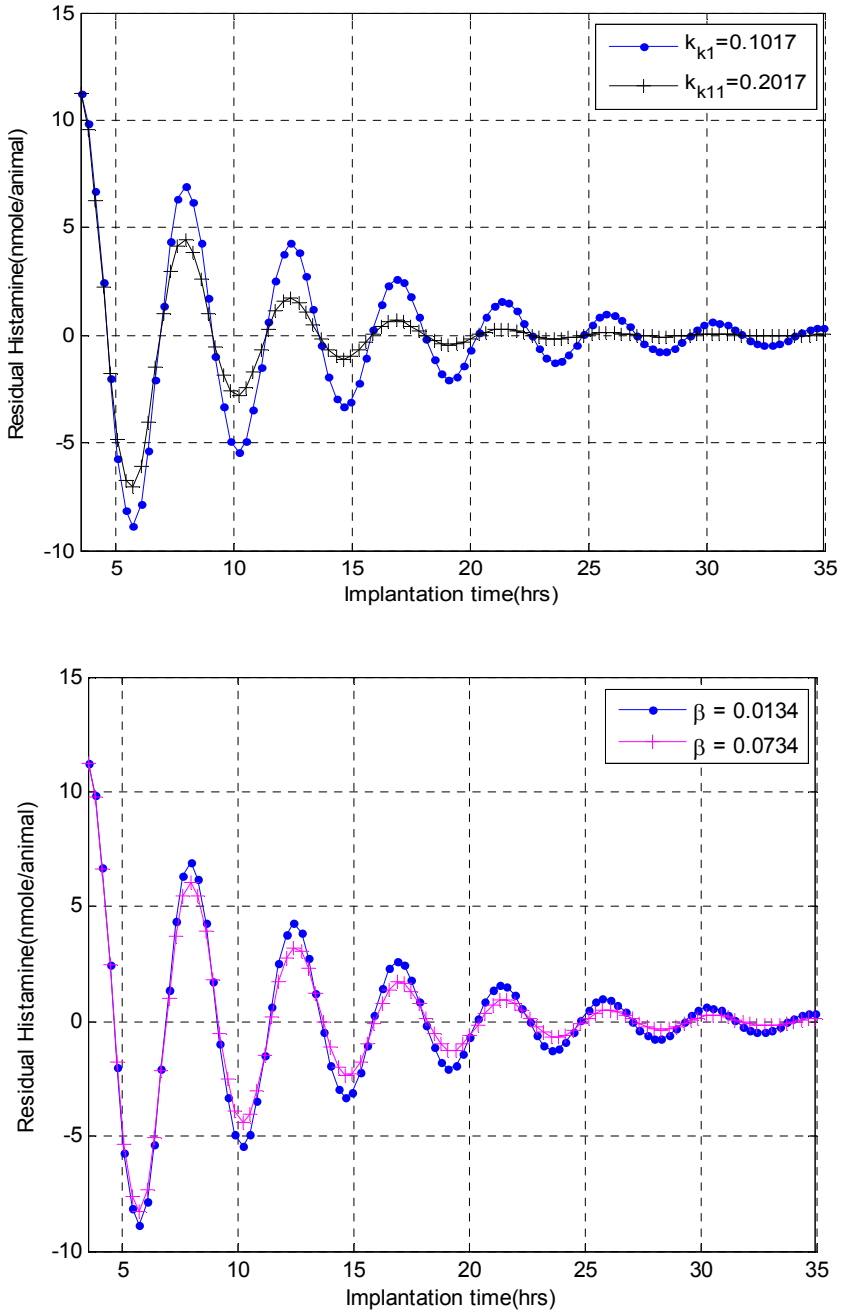

Figure 3: (a) Effects of a self contraction of the external source on residual histamine; (b) Effects of the initial concentration of the oscillation bound on residual histamine.

While Fig. 3 (a) presents the effect of self contraction of the external source on residual histamine, Fig. 3(b) shows the effects of the initial concentration of the oscillation bound of the residual histamine under the influence of time-invariant oscillation frequency. The results depicts that the residual histamine is significantly affected by self-contraction of the external source while initial concentration does have slightly variational effects on the residual histamine. Also, the figures show that the higher the self-contraction of the external source, the lower the residual histamine recorded. The same trend was also recorded on the study of the effects of initial concentration of the oscillation bound on residual histamine.

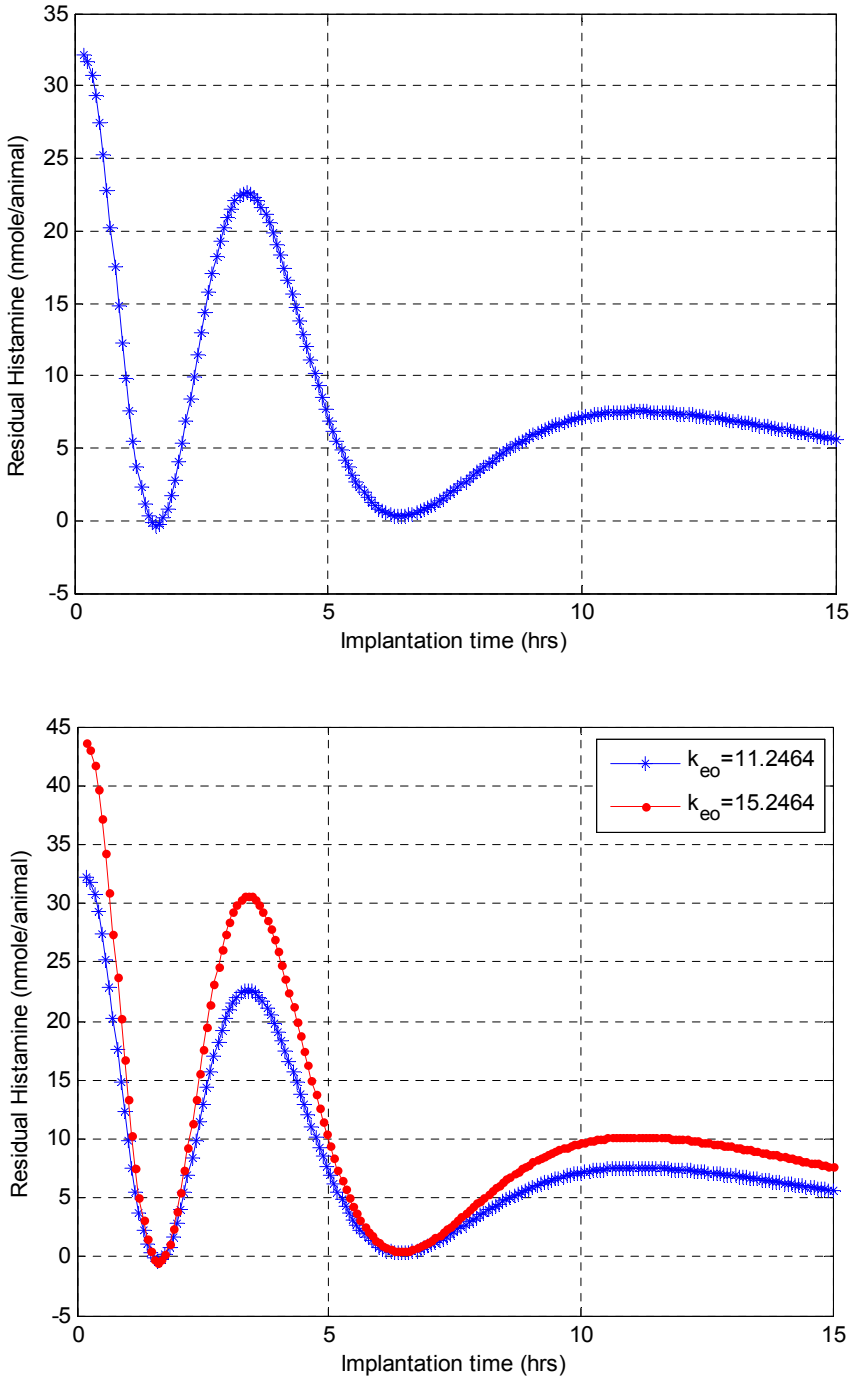

Figure 4: (a) Variation of residual histamine with implantation time; (b) Effects of the initial concentration of the external source on residual histamine.

Fig. 4 shows the variation of residual histamine with time under the effects of time-dependent oscillation frequency. From the figure, it shows the phenomena that residual histamine decreases up to the first two hours can be described as the residual histamine's degranulation from mast cells for histamine releasing. Also, it shows that the number of mast cells is dramatically increased by the immune system shaped as a damped harmonic oscillation after two hours under time-invariant oscillation may be persuasive.

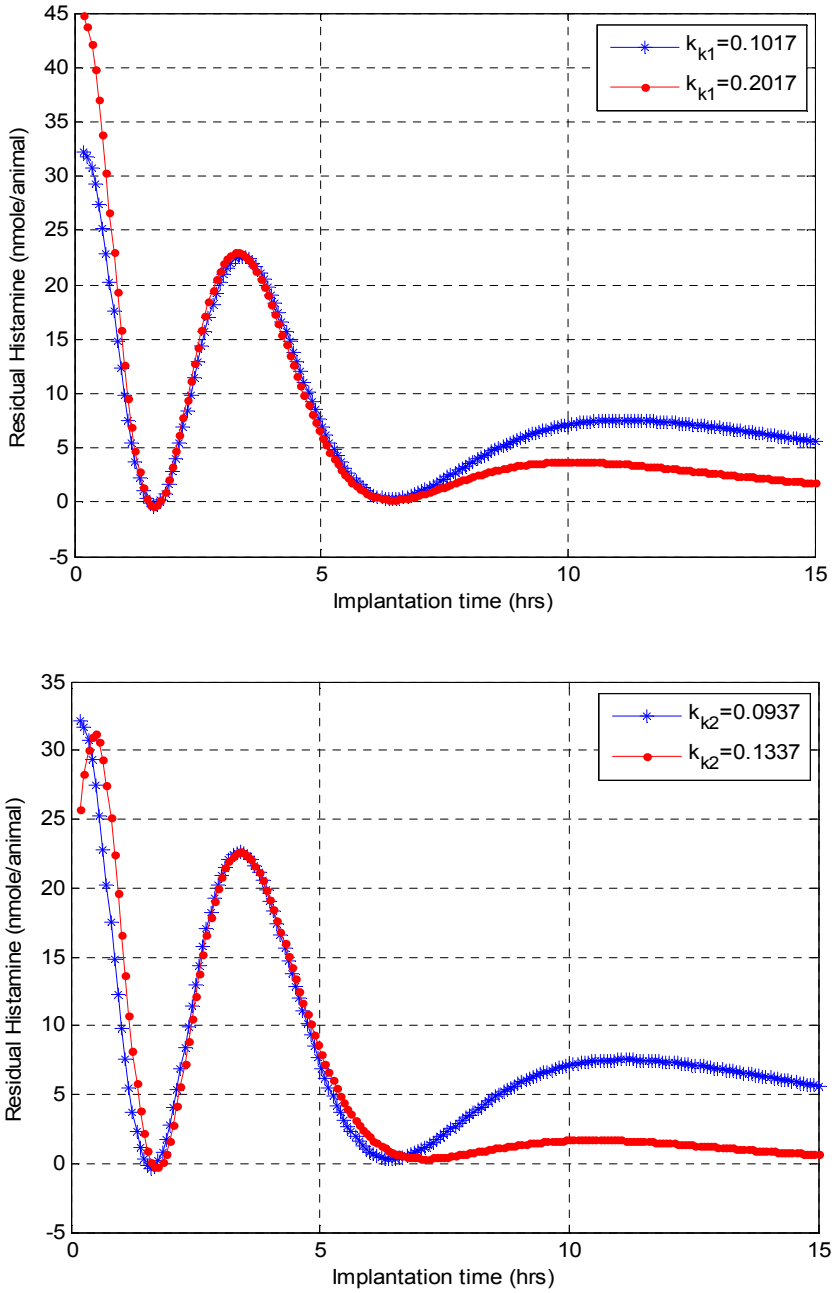

Figure 5: (a) Effects of a self-contraction of the external source on residual histamine; (b) Effects of a contraction rate of the oscillation frequency on residual histamine.

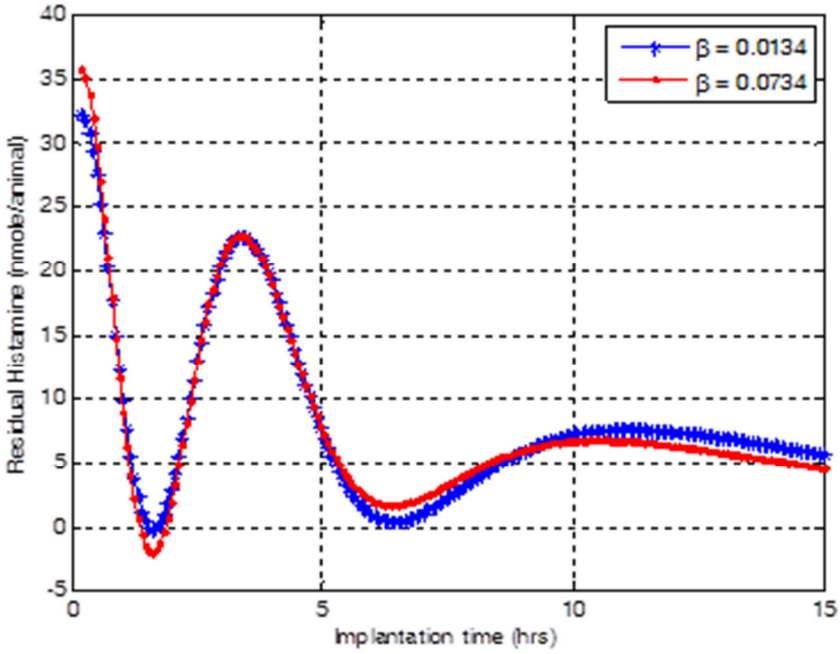

Figure 6: Effects of the initial concentration of the oscillation bound on residual histamine.

The effects of various models parameters on residual histamine under damped oscillation and time-dependent/ time-variant oscillation frequency are presented in Figs. 5 - 6.As pointed out before, the initial concentration of the external source and the self contraction of the external source has direct and significant effects on the residual histamine while initial concentration of the oscillation bound shows inversely proportional relationship on the residual histamine. Comparing Figs. 4-6 with Figs. 2-3, we can see the effects of time-invariant oscillation frequency. It should also be pointed out that the above results correspond to and establish the results of [24].

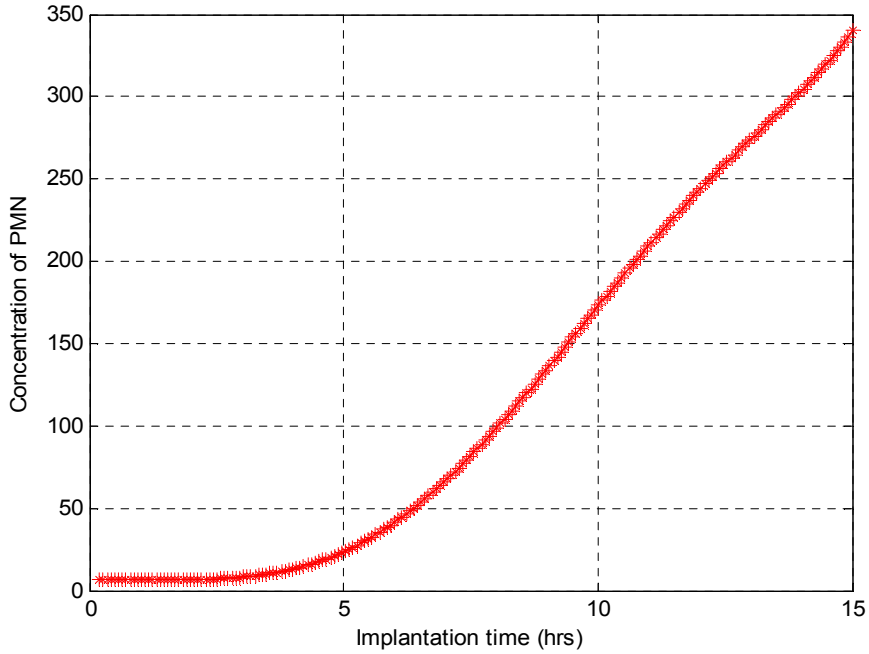

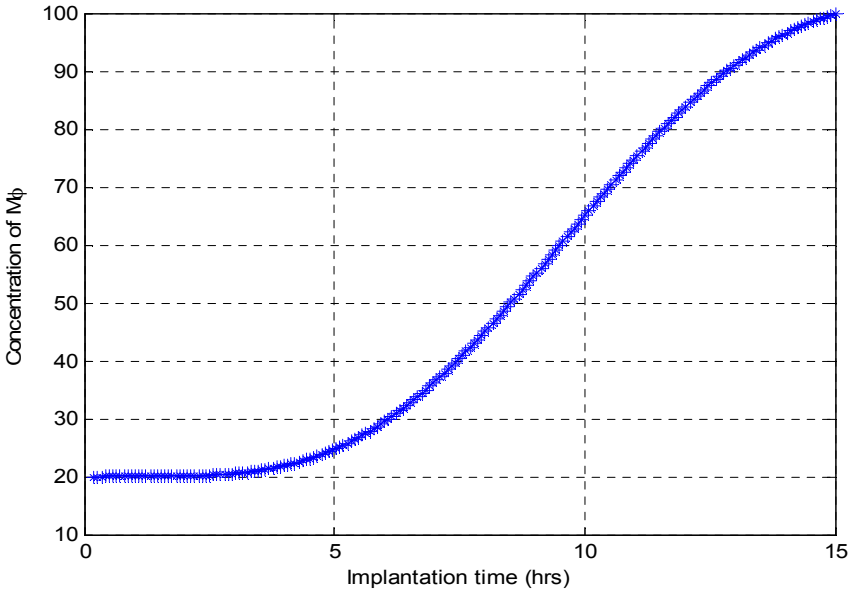

Figure 7: (a) Variation of PMN with implantation time; (b) Variation of macrophages/monocytes with implantation time.

The in silicon estimations for the concentration of PMN and Mϕ are depicted in Fig.6 . The solution given by differential transform method appears to represent and also in good agreement with the previous results given by Discrete Selection Levenberg-Marquardt (DSLM) as submitted by [24]. Also, the differential transform method solution for the recruited phagocytes (PMN and Mϕ) in the peritoneal space estimate closely to the biological observation.

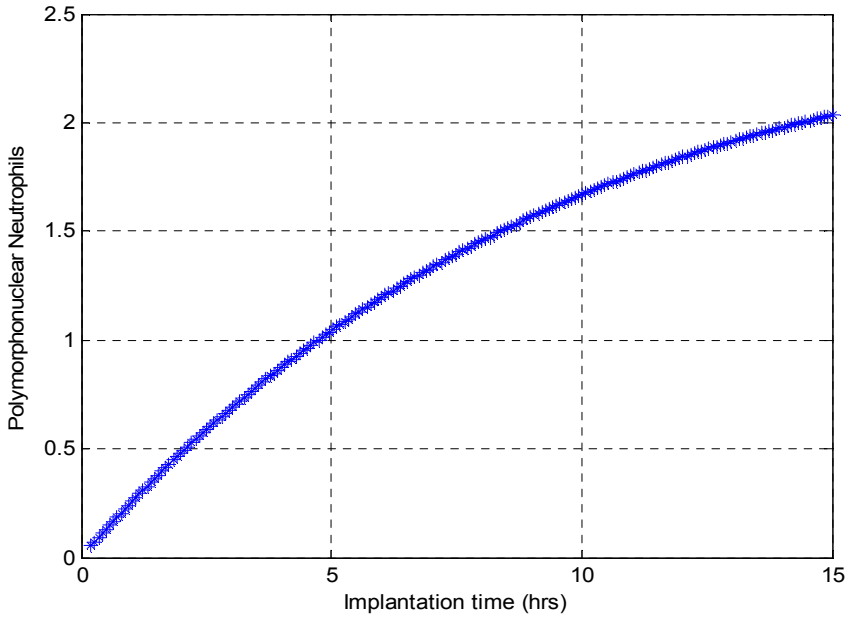

Figure 8: Effects of blocked histamine receptors on PMN.

In order to predict the system behavior under different pertubations, the effects of blocked histamine receptors on polymorphonuclear Neutrophils (PMN) was simulated with DTM solution as shown in Fig. 8, it was observed that PMN was constant for about 3hours of implantation time and then increasing rapidly after then. The same trend was also observed for Mϕ. Then, mathematical tool such as DTM, the influence play a crucial role in reducing the medical implant failure due to the excessive fibrotic responses.

From the above parametric studies, it shows indisputably that the reactions of both the implant on the host blood/tissue and of the host on the implantable device must be understood to avoid health complications to the patient and/or device failure. The degree to which the homeostatic mechanisms are perturbed, the pathophysiological conditions created, and resolution of the inflammatory response can be considered a measure of the host reaction, which ultimately determines the relative compatibility of the device.

The foreign-body response to implanted biomaterials is a very complex series of biochemical events. Initially, there is biofouling of the implant, characterized by protein sheathing, probably initiated by fibrinogen binding. Macrophages bind to specific sites on the protein coat and initiate a series of steps, including formation of multinucleated giant cells. Macrophages also release TGFβ and other inflammatory cytokines. These cytokines transform quiescent fibroblasts into myofibroblasts, which synthesize procollagen via activation of Smad mediators. After crosslinking, the mature collagen and other extracellular matrix proteins contribute to formation of a hypocellular dense fibrous capsule that is hypopermeable to many compounds. Porous substrates and angiogenic growth factors can stimulate formation of microvessels, which, to some extent, can maintain analyte delivery to implanted sensors. It is probably also necessary for other growth factors to act upon immature vessels to mature the fragile microvessels into more robust vessels.

Medical implants provoke unpredicted responses and reactions of the immune system, which are fibrotic capsule formations surrounding the medical device to be specific, wound healing responses start with acute inflammatory response, and then follow with fibrotic tissue reactions. Commonly used implanted biomaterials frequently trigger inflammatory responses accompanied by an accumulation of phagocytic cells (especially macrophages and neutrophils [PMN]) on and adjacent to the implant surface. These inflammatory responses may, in turn, presage serious iatrogenic consequences, such as the "hardening" and degradation of mammary implants, stress cracking of pacemaker leads, and fibrous thickening surrounding many types of implants. The acute and chronic inflammatory responses to these implants are puzzling in view of the inert and nontoxic nature of commonly used polymeric biomaterials. Owing to the fact that protein adsorption is much more rapid than the migration of cells to foreign surfaces, inflammatory cells most likely respond not to the material surface itself but to a chaotic layer of spontaneously adsorbed, partially "denatured" host proteins. Following biological experiments and reports, the diverse components - mast cells, histamine, histamine receptors, and P/E selectins - are involved in the process of phagocyte transmigration with mutual interactions. As one of the major factors comprising phagocyte transmigration, previous studies hypothesized that histamine might play an important role in the recruitment of inflammatory cells to implants. Mast cells are known for the majority source of histamine, and there exists a large amount of mast cells in the peritoneal space. After injecting histamine receptors antagonist, pyrilamine (an H_1 receptor antagonist) and famotidine (an H_2 receptor antagonist) to implanted bio-materials in the mice, it is verified that histamine enhances phagocyte transmigration via both H_1 and H_2 receptors. In addition, the hypothesis that mast cells influence histamine releasing was clarified by the experiment using mast cell-deficient mice. It is also reported that histamine augments the expression of P and E selectins which eventually cause phagocytes' rolling and adhesion on endothelial cells. The analytical modeling does not only provides critical clues to recognize current knowledge of fibrosis development but also enables the prediction of yet-to-be observed biological phenomena. Also, in-depth understanding of the foreign body responses and its computational modelling will disclose the contributing components and help to predict the evolution, which would eventually lead to reduced failure rate of implantation. Understanding the biological nature of the foreign-body response is necessary for development of longer-term and more accurate biosensing devices. Reactions of both the implant on the host blood/tissue and of the host on the implantable device must be understood to avoid health complications to the patient and/or device failure. The degree to which the homeostatic mechanisms are perturbed, the pathophysiological conditions created, and resolution of the inflammatory response can be considered a measure of the host reaction, which ultimately determines the relative compatibility of the device.

Conclusion

In this work, approximate analytical solutions have been developed for phagocyte transmigration to foreign body responses in biomaterial implantation using differential transformation method. The analytical solutions were used to study the effect of various model parameters on phagocyte transmigration to foreign body responses in biomaterial implantation. The results of the analytical solutions were compared to the results of the previous studies and good agreements were reached. The analytical solution can serve as a benchmark for the numerical solution. Based on the symbolic nature of the analytical solution developed in this work, they provide better understanding of relationship between the physical quantities of the problem investigated.

References

[1] L. Zhang, Z. Cao, T. Bai, L. Carr, J. Ella-Menye, C. Irvin, B. D. Ratner, S. Jiang. Zwitterionic hydrogels implanted in mice resist the foreign-body reaction, Nature Biotechnology, 31, 553–556, 2013

[2] L. Tang, T.A. Jennings, J.W. Eaton. Mast cells mediate acute inflammatory responses to implanted biomaterials. Proc Nat Acad Sci. 95, (1998), 8841–8846.

[3] W. K. Ward,. A review of the foreign-body response to subcutaneously-implanted devices: The role of macrophages and cytokines in biofouling and fibrosis. J Diabetes Sci Technol.2, (2008), 768–777.

[4] B. Rolfe, J. Mooney, B. Zhang, S. Jahnke, S.J. Le, Y.Q. Chau, Q. Huang, G. Wang, H. Campbell, J. Campbell. The fibrotic response to implanted biomaterials: Implications for tissue engineering. In: Eberli D., editor. Regenerative Medicine and Tissue Engineering: Cells and Biomaterials. Rijeka, Croatia: InTech Publishing; 2011.

[5] J. Xue, J. Gao, L. Tang. A hybrid computational model for phagocyte transmigration. In: BioInformatics and BioEngineering, 8th IEEE International Conference On. Boston: IEEE; 2008. p. 1–6.

[6] J. Su, M. Todorov, H.P. Gonzales, L. Perkins, H. Kojouharov, H. Weng, L. Tang. A predictive tool for foreign body fibrotic reactions using 2-dimensional computational model. Open Access Bioinformatics.3, (2011), 19–35.

[7] J. Su, M. Todorov, H.P. Gonzales, L. Perkins, H. Kojouharov, H. Weng, L. Tang. A mathematical model for foreign body reactions in 2D.Int J Comput. Math. 88, (2011), 610–633.

[8] J. Yang, J. Su, L. Owens, A. Ibraguimov, L. Tang. A computational model of fibroblast and macrophage spatial/temporal dynamics in foreign body reactions. J Immunol. Methods. 397 (1–2), 2013, 37–46.

[9] L. Tang, J.W. Eaton. Natural responses to unnatural materials: A molecular mechanism for foreign body reactions. Mol Med. 6 (5), 1999, 351–358.

[10] J. Zdolsek, J. Eaton, L. Tang. Histamine release and fibrinogen adsorption mediate acute inflammatory responses to biomaterial implants in humans. J Transl. Med. 5(1), 2007 31.

[11] L. Tang, W. Jiang, S.E. Welty. The participation of p- and e-selectins onbiomaterial-mediated tissue responses. J Biomed Mater Res. 62 (4), 2002, 471–477.

[12] M. Kang, J.X. Gao, L. Tang. Computational modeling of phagocyte transmigration during biomaterial-mediated foreign body responses. In:Bioinformatics and Biomedicine (BIBM), 2010 IEEE International Conference On. Hong Kong: IEEE; 2010. p. 609–612.

[13] L. Tang, Y. Wu, R.B. Timmons. Fibrinogen adsorption and host tissue responses to plasma functionalized surfaces. J Biomed Mater Res. 42 (1) 1998, 156–163.

[14] P.T. Thevenot, D.W. Baker, H. Weng, M.W. Sun, L. Tang. The pivotal role of fibrocytes and mast cells in mediating fibrotic reactions to biomaterials. Biomaterials. 32 (33), 2011, 8394–8403.

[15] S. Yamasaki, ST. Regulation of mast cell activation through fcepsilonri. ChemImmunol Allergy. 87, 2005, 22–31.

[16] J.K. Zhou, Differential transformation and its applications for electrical circuits, Huazhong University Press, Wuhan, China. (1986).

[17] A. Arikoglu, and I. Ozkol, Vibration analysis of composite sandwich beams with viscoelastic core by using differential transform method, Compos Struct. 92, (2010), 3031-3039

[18] Z. Odibat, C. Bertelle, M. A. Aziz-Alaoui, and G.H.E. Duchampd, A multi-step differential transform method and application to non-chaotic or chaotic systems. Comput. Math. Appl. 59, (2010), 1462-1472

[19] P. Salehi, H. Yaghoobi, and M. Torabi, Application of the differential transformation method and variational iteration method to large deformation of cantilever beams under point load, Journal of Mechanical Science and Technology, 26, (2012), 2879–2887

[20] M. Madani, M. Fathizadeh, Y. Khan and A. Yildirim, "On the coupling of the homotopy perturbation method and Laplace transformation," J. Mathematical and Computer Modelling, 53 (9-10), (2011), 1937-1945.

[21] D. Carlos, A. Sa-Nunes, L. de Paula, C. Matias-Peres, M.C. Jamur, C. Oliver, M.F. Serra, M.A. Martins, L.H. Faccioli. Histamine modulates mast cell granulation through an indirect mechanism in a model ige-mediated reaction. Eur J Immunol. 36 (6), 2006, 1494–1503.

[22] C.K Chen, and S.H. Ho, Solving partial differential equations by two dimensional differential transform. Appl. Math. Comput. 106, 1999, 171-179.

[23] M. Thongmoon, and S. Pusjuso, The numerical solution of differential transform method and Laplace transform method for a system of differential equations. Nonlinear Anal. Hybrid Syst.4, 2010, 425-431

[24] M. Kang, L. Tang, J. Gao, Computational modeling of phagocyte transmigration for foreign body responses to subcutaneous biomaterial implants in mice, BMC Bioinformatics 111 (17), 2016, 1-13.